Chinese Journal of Polymer Science Vol. 33, No. 1, (2015), 153–162

Chinese Journal of Polymer Science

Balance of Polyacrylate-Fluorosilicone Block Copolymers as Icephobic Coatings*

Kai-qiang Zhang[a†], Jing-zhe Cai[a†], Xiao-hui Li[a], Hui Li[b], Yun-hui Zhao[a**] and Xiao-yan Yuan[a**]

[a] *School of Materials Science and Engineering, and Tianjin Key Laboratory of Composite and Functional Materials, Tianjin University, Tianjin 300072, China*

[b] *School of Chemistry and Chemical Engineering, Shandong Key Laboratory of Fluorine Chemistry and Chemical Engineering Materials, University of Jinan, Jinan 250022, China*

Abstract Polyacrylate-fluorosilicone block copolymers, namely, polyacrylate-*b*-polydimethylsiloxane and polyacrylate-*b*-polymethyltrifluoropropylsiloxane were synthesized for fabricating icephobic coatings. The surface morphology and chemical composition of the block copolymers were characterized by atomic force microscopy and X-ray photoelectron spectroscopy, suggesting that the fluorosilicone blocks aggregated on the top of the copolymer surfaces. Results of water contact angles and ice shear strength demonstrated a certain amount adding of methacryloisobutyl polyhedral oligomeric silsesquioxane could lead to the decrease of contact angle hysteresis and increase of surface roughness, consequently resulting in significant reduction of the ice adhesion strength. Therefore, the block copolymers with the combined advantages of silicone and fluoropolymers could be potentially applied as icephobic coatings.

Keywords: Block copolymer; Polydimethylsiloxane; Polymethyltrifluoropropylsiloxane; Polyacrylate; Icephobicity.

INTRODUCTION

Considerable interests and extensive investigations have been conducted to focus on anti-icing surfaces *via* eliminating ice formation or reducing ice adhesion[1–6]. Because of the low surface energy, fluorine/silicon-containing polymers have been widely utilized to prepare icephobic and non-wetting coatings for decades. Taking advantage of the above mentioned two types of materials, superhydrophobic coatings enabled by micro/nano-scaled surface roughness were often considered as an alternative strategy for water-repellency or anti-icing, presenting good anti-icing performances in combating water accumulation before water freezes[1, 5, 6].

It is well-known that certain surface roughness triggered by its interface microcracks is crucial to superhydrophobic surfaces[6], however, this also can be the reason for the questionable use of superhydrophobic surfaces in the field of icephobic coatings[2, 7–10]. Susoff *et al*. debated that the ice adhesive strength was enhanced by the increased surface roughness, and relatively rougher surfaces adhered stronger to ice than the smoother ones did[2]. Without sufficiently large voids at the interface, some superhydrophobic surfaces could have strong ice adhesion strength[9]. Interestingly, uniform nano-scaled surfaces obtained by the self-assembly and self-aggregation of block copolymers may offer the surface a nanosized roughness that could be beneficial to

* This work was financially supported by the National Natural Science Foundation of China (Nos. 51273146 and 51103061) and Natural Science Foundation of Tianjin, China (No.14ZCZDGX00008).
** Corresponding authors: Yun-hui Zhao (赵蕴慧), E-mail: zhaoyunhui@tju.edu.cn
Xiao-yan Yuan (袁晓燕), E-mail: yuanxy@tju.edu.cn
† Kai-qiang Zhang and Jing-zhe Cai contributed equally to this work.
Received May 30, 2014; Revised June 18, 2014; Accepted July 15, 2014
doi: 10.1007/s10118-015-1563-9

anti-icing[11].

Polysiloxane is usually applied to generate anti-icing surfaces due to its notable properties such as low glass transition temperature and low surface energy[1, 4, 12]. Especially, polydimethylsiloxane (PDMS) has been extensively associated with other polymeric units to form anti-icing materials, attributed to its low free surface energy (22 $mN \cdot m^{-1}$) and low glass transition temperature (−123 °C)[13, 14]. Zhu *et al*. observed that the ice adhesion can be reduced dramatically by preparation of silicon-oil-infused PDMS coatings[13]. Significantly, smaller rate of ice accumulation was detected in the PDMS/modified nano-silica insulator hybrid coating[14]. Our previous work indicated that ice adhesion strength was decreased by the contribution of PDMS in the polyacrylate-*b*-PDMS or polyacrylate-*g*-PDMS copolymers with longer PDMS side chains[11].

Another effective route to reduce ice adhesion strength has been focused on the fluorinated polymers. Owing to the surface self-organization and self-assembly of fluorinated segments, the fluorinated polymer can endow a surface with low surface energy, exhibiting high contact angles for wetting liquids[15]. Naturally, increased attention has been devoted to the comprehensive combination of fluorinated groups and siloxane segments into synthetic materials[16–20]. Several approaches have been proposed to synthesize fluorosilicone polymers, *i.e.* by fluorinated siloxanes[16, 17] or by copolymerizing fluorinated alkyl side groups and siloxane moieties modified acrylate monomers[18–21]. The self-assembly behaviors of polysiloxane segments and fluorinated block copolymers play a significant role in the generation of low-energy surfaces, and the microphase separation behavior generally occurs on the surfaces of the block polymers, thus, affecting their surface properties[18, 19, 21]. Higher advancing and receding contact angles for water could be obtained in the case of synergism between surface enrichment of fluorine and silicon[18]. A well-known fluorinated polysiloxane is polymethyltrifluoropropylsiloxane (PMTFPS), presenting good fuel and oil resistance along with weather and thermal stability, low polarity, low-temperature flexibility and low surface energy[16, 17].

Comparison between poly(methyl methacrylate) (PMMA)-*g*-PDMS and PMMA-*g*-PMTFPS graft copolymers have been investigated to elucidate the role of surface energy in these materials[17]. However, to the best of our knowledge, few literatures have reported the comparison of PDMS-containing and PMTFPS-containing fluorosilicone block copolymers for anti-icing. Followed our previous work[11], comparison between polyacrylate-*b*-PDMS and polyacrylate-*b*-PMTFPS block copolymers were investigated here. The block copolymers were synthesized by employing PDMS-MAI and PMTFPS-MAI as macroazoinitiators, respectively. 2,2,3,3,4,4,5,5,6,6,7,7- Dodecafluoroheptyl methacrylate (DFHMA) was introduced to build fluorosilicone block structures. In addition, methacryloisobutyl polyhedral oligomeric silsesquioxane (MAPOSS) was used to mediate surface morphology. The polymer surface characterizations including microphase morphology, surface chemical composition, contact angles and ice shear strength were investigated, and the comparison of the copolymers in icephobic properties was emphasized.

EXPERIMENTAL

Materials

α,ω-Dihydrogen-terminated capped PDMS of about 5000 molecular weight was supplied by Hangzhou Silong Material Technology Co., Ltd., China. *α,ω*-Dihydrogen-terminated polymethyltrifluoropropylsiloxane (H-PMTFPS-H) with relative molar mass of about 5000 was obtained from Shanghai Silicon Mountain Macromolecular Materials Co., Ltd., China. 4,4-Azobis(4-cyanovaleric acid) (ACVA) and platinum divinyltetramethyldisiloxane complex in xylene were purchased from Sigma Aldrich. MAPOSS was purchased from Hybrid Plastics, Inc., USA, and used as received. DFHMA was supplied by Xeogia Fluorin-Silicon Chemical Co. Ltd, China. The monomers including methylmethacrylate (MMA), *n*-butyl acrylate (*n*BA) and hydroxyethyl methacrylate (HEMA) as well as solvents including dichloromethane (DCM), *N,N*-dimethyl formamide (DMF), *etc*. were also supplied by Tianjin Kemiou Chemical Reagent Co., Ltd., China, and dried before use. *α,α,α*-Trifluorotoluene (TFT) was purchased from Tianjin Heowns Biochem Technologies LLC, Tianjin, China.

Synthesis

Polyacrylate-*b*-PDMS were synthesized by initiation of macroazoinitiators (PDMS-MAI) and polymerization of monomers including MMA, *n*BA, HEMA, DFHMA and MAPOSS, for the purpose of obtaining different samples (Table 1). Detailed synthesis can be found in our previous report[11]. For comparison, polyacrylate-*b*-PMTFPS block copolymer was also synthesized by free radical polymerization of MMA, *n*BA and HEMA with PMTFPS-MAI as macroazoinitiator. The structure of the copolymers is illustrated in Scheme 1. The resulting polyacrylate-*b*-PMTFPS copolymer was precipitated in ethanol and vacuum-dried at 40 °C. The compositions of the prepared block copolymers are shown in Table 1.

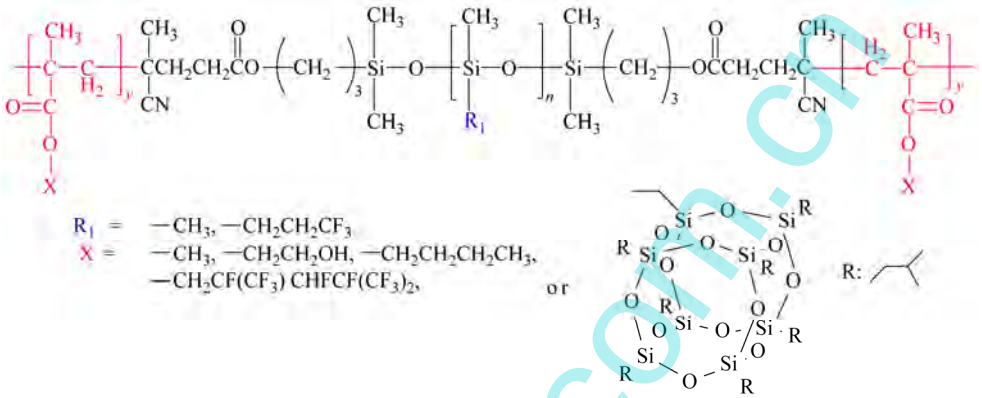

Scheme 1 Structure of fluorosilicone acrylate block copolymers

Table 1. Composition and relative molar mass of the prepared fluorosilicone acrylate block copolymers

Sample	PDMS-MAI (g)	PMTFPS-MAI (g)	Monomer (g)					M_n ($\times 10^4$)	PDI
			MMA	BA	HEMA	DFHMA	MAPOSS		
PDMS-*b*-AC	4.93	–	5.5	4.5	1.5	–	–	5.00	2.15
PDMS-*b*-FAC	6.43	–	5.5	4.5	1.5	3.5	–	2.96	2.47
PDMS-*b*-FPAC	7.07	–	5.5	4.5	1.5	3.5	1.5	3.77	2.33
PMTFPS-*b*-AC	–	4.93	5.5	4.5	1.5	–	–	1.23	1.81

Preparation of the Copolymer Films

The copolymer films were prepared by spraying the copolymer solutions in TFT with a concentration of 10 wt% on polished aluminum plates (20 mm × 20 mm), allowing the solvent to evaporate completely at room temperature in air. A given amount of the curing agent (hexamethylene diisocyanate trimer) was supplied. The prepared copolymer films were annealed at 130 °C for 3 h.

Characterizations

Gel permeation chromatography (GPC) traces were obtained with a Waters 1515 Isocratic HPLC pump equipped with a Waters 2414 refractive index detector. The flow rate was 1 mL of THF/min at 40 °C. The relative molar mass and polydispersity index (PDI) of the prepared fluorosilicone acrylate block copolymers are summarized in Table 1.

Fourier transform infrared spectra (FTIR) were recorded in a Perkin-Elmer Spectrum 100. Polymer films were cast on KBr pellets from TFT for the measurement. The solid nuclear magnetic resonance (^{29}Si-NMR) measurement was carried out in Varian machines (INOVA500MHz and Infinity plus 300WB, USA). Proton-nuclear magnetic resonance (^{1}H-NMR) analysis was carried out in Varian machines (INOVA 500 MHz and Infinity plus 300WB, USA) by dissolving the samples in deuteriochloroform.

Differential scanning calorimetric analysis (DSC) was performed with a Perkin-Elmer Diamond differential scanning calorimeter under a dry nitrogen atmosphere with a heating rate of 10 K/min and heated from −150 °C to 220 °C.

Surface composition by X-ray photoelectron spectroscopy (XPS) was estimated using a Perkin-Elmer PHI 5000C ECSAX-ray photoelectron spectroscope in ultra-high vacuum with Al K radiation (1486.6 eV) operating at 24.2 W under a vacuum less than 5×10^{-8} Torr at 45°. The tested area was a circle in 100 μm diameter.

Atomic force microscope (AFM) images were obtained using tapping mode on a CSPM5500A machine (Being Nano-Instruments Ltd., Guangzhou, China) equipped with E-type vertical engage piezoelectric scanner. The AFM samples were prepared by spin-coating the solution of block copolymers (10 wt% in TFT) onto freshly cleaved silicon wafer surfaces, and then dried at 130 °C for 3 h.

Static contact angle, advancing angle and receding angle were measured using a JC2000D contact angle meter (Shanghai Zhongchen Equipment Ltd., China). The surface energy of polymers was evaluated by measuring static water and hexadecane contact angles on the surface.

Ice shear strength was measured within a custom-made humidity-controlled chamber in a low-humidity nitrogen atmosphere equipped with a force transducer (Model ZP-500, Imada, Japan) in a push mode. The push velocity was controlled at a constant rate of 0.5 mm/s by using a motion stage (Liansheng, Jianxi Province, China). Cylindrical glass columns with an inner diameter of 10 mm were made by cutting glass tubes with a well-polished end and treated with tridecafluoro-1,1,2,2-tetrahydrooctyl trichlorosilane for at least 24 h. A certain amount of water was filled in glass columns which were mounted on the samples held on the cooled plate. The temperature of the cooling plate was cooled at a rate of 2 K/min to the target temperature and frozen at −15 °C for 3 h before tests. The push force was recorded until ice detached for determining the ice shear strength ($n > 5$) by dividing the area 78.5 mm^2 between ice and coating surface.

RESULTS AND DISCUSSION

The main purpose of this research is to assess the icephobic properties of polyacrylate-*b*-PDMS and polyacrylate-*b*-PMTFPS with different components and compositions. Especially, we initially explored two series fluorosilicone polymers for building anti-icing coatings and the synergistic effect of fluorine/silicone segments. Considering as the important factors for icephobic behaviors, the microphase-separated structure and the surface chemical composition were analyzed to make clear the effects of fluorine/silicone segments on the wettability and ice adhesion strength of the obtained copolymer surfaces.

Chemical Structures of the Prepared Fluorosilicone Polyacrylate Block Copolymers

The chemical structures of the prepared copolymers polyacrylate-*b*-PDMS and polyacrylate-*b*-PMTFPS were confirmed by analyses of FTIR, ^{1}H-NMR and ^{29}Si-NMR spectra. As shown in Fig. 1, the absorption peak in the range of 1000–1150 cm^{-1} was assigned to Si—O—Si asymmetric stretching vibrations that appeared in all the FTIR curves. Appearance of the peak at 1735 cm^{-1} was due to the existence of C=O stretching, and the absorption peak at 2960 cm^{-1} was assigned to ν ($-CH_3$). The above results indicated the successful polymerization of acrylate monomers (MMA and *n*BA) into the block copolymers.

As shown in Fig. 2, compared with PDMS-*b*-FAC (Fig. 2a), the ^{29}Si-NMR spectrum of PDMS-*b*-FPAC (Fig. 2b) showed two groups of Si atoms, exhibiting two different chemical shifts. One shift from −65 to −72 was due to the $SiO_{1.5}$ unit in MAPOSS, while the other from −20 to −24 to the $-O_2Si(CH_3)_2$ unit originated from PDMS. The results of Fig. 2 demonstrated the successful introduction of MAPOSS to the block copolymer PDMS-*b*-FPAC.

The difference between PMTFPS-*b*-AC and PDMS-*b*-AC was confirmed by ^{1}H-NMR spectra as shown in Fig. 3. In the ^{1}H-NMR spectrum of PMTFPS-*b*-AC (Fig. 3b), the resonances at δ = 1.96 and 2.15 were associated with the protons of the $-CH_2-CH_2-CF_3$ groups, distinguishing from PDMS-*b*-AC (Fig. 3a).

DSC Analysis

The thermal transitions of the prepared block copolymers were investigated by DSC as shown in Fig. 4. The DSC thermograms of PDMS-*b*-AC, PDMS-*b*-FAC and PDMS-*b*-FPAC showed two glass transition temperatures, one at low temperatures (from −130 °C to −120 °C) and the other at higher temperatures (from 60 °C to 70 °C), corresponding to PDMS and polyacrylate-enriched domain, respectively, and suggesting

possible incompatibility between PDMS and polyacrylate blocks in the copolymers. Similar phenomena were also found in our previous report[11] and the references[18, 19]. An endothermic peak was also found near −50 °C in the PDMS-*b*-FAC thermogram, owing to PDMS melting. However, the melting temperature of PDMS was not detected for PDMS-*b*-FPAC due to the introduction of MAPOSS, and neither for PDMS-*b*-AC because of high molecular weight of the copolymer and the small percentage of PDMS. For PMTFPS-*b*-AC, T_{g1} associated with PMTFPS blocks was found at −66.8 °C and another glass transition temperature at 55.2 °C contributed to polyacrylate, which is coincident with the early results[16, 17]. The result indicated that potential microphase separation might happen in the prepared PDMS-*b*-AC, PDMS-*b*-FAC, PDMS-*b*-FPAC and PMTFPS-*b*-AC block copolymers.

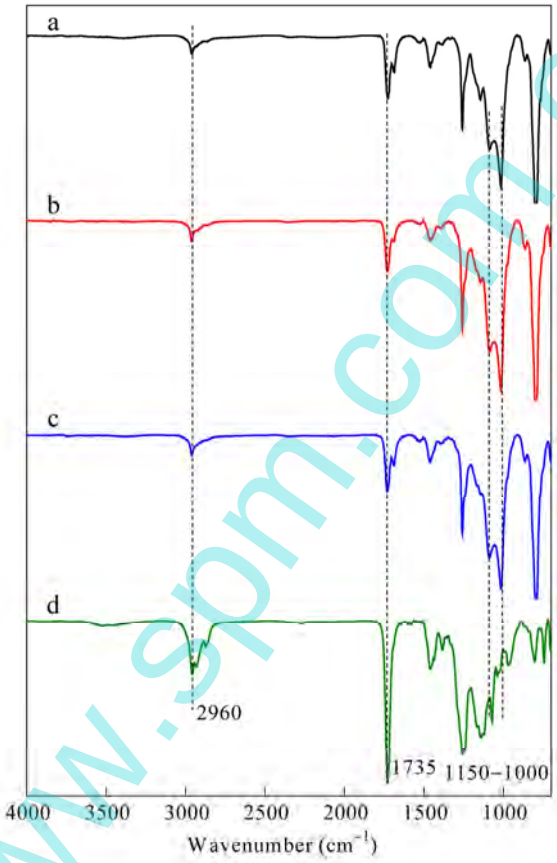

Fig. 1 FTIR spectra of the copolymer films: (a) PDMS-*b*-AC, (b) PDMS-*b*-FAC, (c) PDMS-*b*-FPAC and (d) PMTFPS-*b*-AC

XPS Analysis

The surface chemical compositions of the copolymers surfaces were characterized by XPS. The percentages of carbon, oxygen, and silicon as well as atomic relative ratio estimated from the XPS survey spectra are summarized in Table 2. The characteristic signal intensity of silicon increased significantly to 18.6% with the introduction of MAPOSS in copolymers PDMS-*b*-FPAC due to the movement of larger POSS groups toward air-side surfaces and the driven segregation of siloxane caused by enhanced microphase separation. Owing to the fluorinated polysiloxane structure, the migration of $-CF_3$ groups towards outside in PMTFPS-*b*-AC copolymers was much more easier than that in polyacrylate-*b*-PDMS copolymers, enriching fluorine segments on the surface to 25.6%, and F/Si atom ratio achieved the highest value 2.10. All the results indicated that fluorine-containing and silicon-containing groups aggregated easily onto the film surface due to microphase separation.

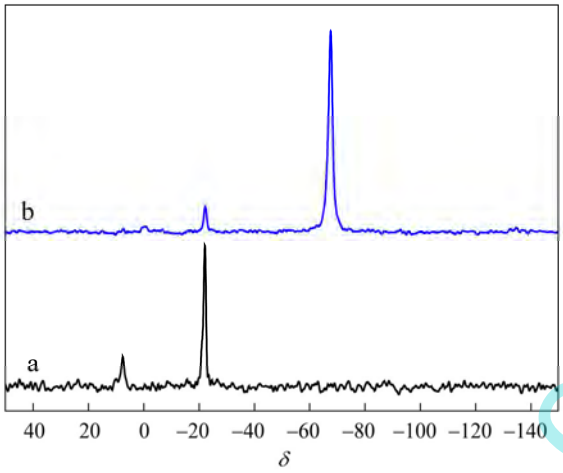

Fig. 2 ^{29}Si-NMR spectra of PDMS-*b*-FAC (a) and PDMS-*b*-FPAC (b)

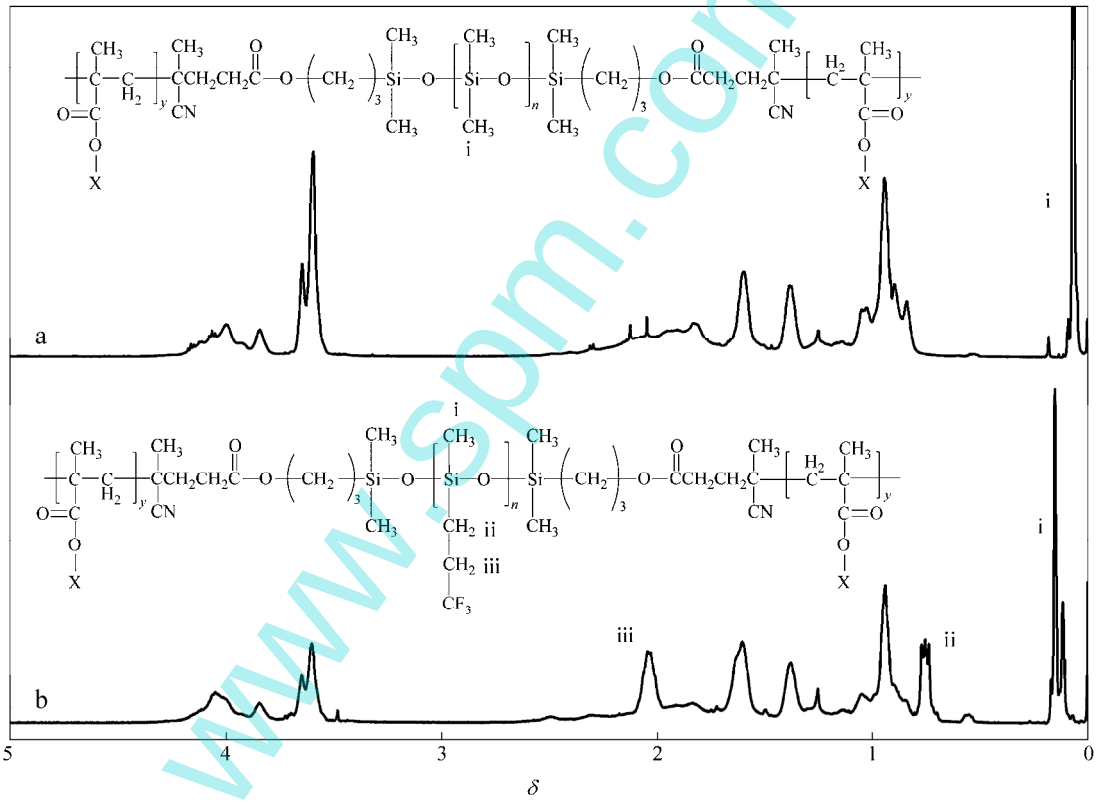

Fig. 3 ^{1}H-NMR spectra of PDMS-*b*-AC (a) and PMTFPS-*b*-AC (b)

Table 2. Element composition of the copolymer surface detected by XPS

Sample	C (atomic %)	O (atomic %)	F (atomic %)	Si (atomic %)	F/Si
PDMS-*b*-AC	57.5	31.2	–	11.3	–
PDMS-*b*-FAC	61.7	23.0	3.1	12.2	0.25
PDMS-*b*-FPAC	55.7	24.7	1.3	18.6	0.07
PMTFPS-*b*-AC	46.6	15.6	25.6	12.2	2.10

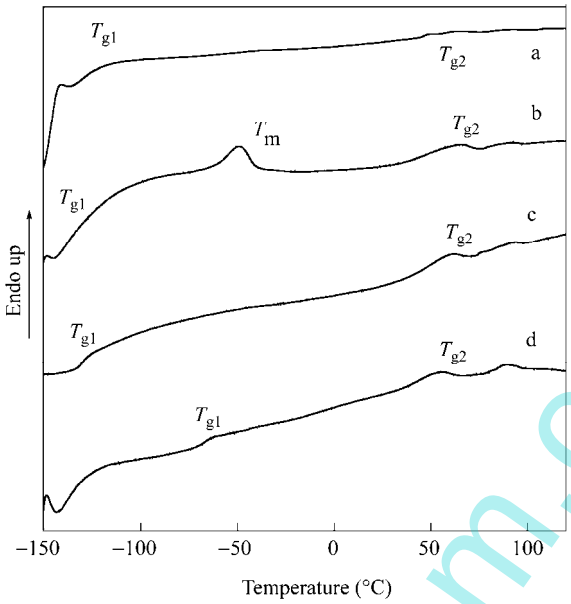

Fig. 4 DSC thermograms of PDMS-*b*-AC (a), PDMS-*b*-FAC (b), PDMS-*b*-FPAC (c) and PMTFPS-*b*-AC (d)

Surface Morphology

As shown in Fig. 5, the four samples exhibited different morphologies in the AFM images. It can be suggested that the bright area (yellow) in the topography images is the PDMS-rich phase and fluorine segments, while the dark area (brown) could be referred to the polyacrylate-rich phase that tended to attach on the hydrophilic substrate. As shown in Figs. 5(a, b, c), microphase separation in the copolymers was detected, and PDMS chains and fluorine segments protuberated outwards forming a rough surface. Compared with PDMS-*b*-AC (Fig. 5a), dark spots referred to polyacrylate phase were observed in PDMS-*b*-FAC (Fig. 5b) due to the further surface segment segregation of fluorine segments with the addition of DFHMA. Attributed to the migration of POSS groups, more distinct phase separation was observed in PDMS-*b*-FPAC (Fig. 5c). No clearly microphase-separated morphology on the surfaces of PMTFPS-*b*-AC (Fig. 5d) was observed, which agreed well with the reference[17]. It can be assumed that the polyacrylate-*b*-PDMS copolymers were easier to bring about microphase separation structures rather than fluorinated polysiloxane (PMTFPS-*b*-AC) in our experiments, because of the more notable thermodynamic incompatibility between polysiloxane and fluorinated polyacrylate blocks. The results of AFM agreed well with the XPS analysis. Additionally, a certain degree of microphase separation appeared in AFM phase images was coincident with analyses about the multiphase detected by DSC.

Along with the migration and self-segregation of low surface energy chains, surface morphologies exhibited significant characteristics on the given surfaces. Compared with PDMS-*b*-AC, the root-mean-square roughness (R_q in Table 3) of PDMS-*b*-FAC film increased with the addition of the DFHMA content, which was consistent with the reference[21]. A remarkable increase in surface roughness to 3.07 nm appeared for sample PDMS-*b*-FPAC, which corresponded well to the added MAPOSS in this copolymer[11]. The minimum surface roughness to 1.88 nm was observed for sample PMTFPS-*b*-AC, and the decrease in surface roughness correlated well with its microphase separation behavior. According to Susoff 's study, relatively rough surfaces adhered stronger to ice than smoother ones[2]. Jung *et al.* also reported that nanometer-scale smooth surfaces with low roughness (1.4–6 nm) showed much better icephobic properties than superhydrophobic surfaces[10]. Hence, samples with small nano-scaled surface roughness in our experiment are expected to have better icephobic performances.

Table 3. Surface energy, water contact angles, and roughness of the copolymer films

Sample	Surface energy (mN/m)	Static contact angle (°)	Advancing contact angle (°)	Receding contact angle (°)	Contact angle hysteresis (°)	R_q (nm)
PDMS-*b*-AC	27.2 ± 0.5	103.7 ± 0.7	108.5 ± 0.6	74.6 ± 1.1	33.9 ± 2.4	2.04
PDMS-*b*-FAC	25.2 ± 1.0	105.0 ± 0.2	108.9 ± 1.6	77.4 ± 0.8	31.5 ± 0.7	2.17
PDMS-*b*-FPAC	25.8 ± 0.3	106.6 ± 0.2	111.9 ± 3.1	86.4 ± 0.5	24.4 ± 1.2	3.07
PMTFPS-*b*-AC	24.4 ± 0.5	102.7 ± 0.1	106.8 ± 0.1	70.3 ± 1.5	36.5 ± 1.1	1.88

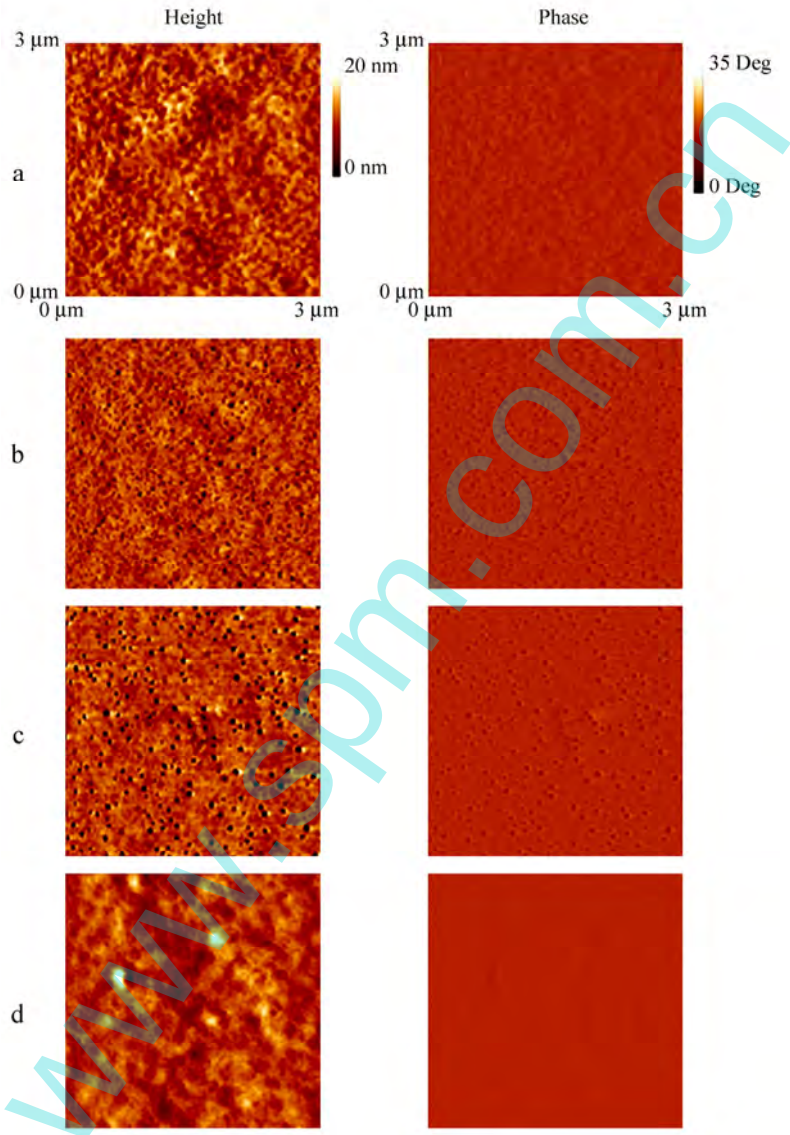

Fig. 5 AFM topography and phase images of PDMS-*b*-AC (a), PDMS-*b*-FAC (b), PDMS-*b*-FPAC (c) and PMTFPS-*b*-AC (d)

Contact Angles and Surface Energy

Static water contact angles (WCA), advancing (θ_a), and receding (θ_r) contact angles, and contact angle hysteresis (CAH) are summarized in Table 3. As we all know, both surface morphology and composition have influences on the WCA, θ_a and θ_r values. All the fluorosilicone polyacrylate block copolymers films were hydrophobic, exhibiting WCA between 102° and 106°. Sample PDMS-*b*-FAC showed higher WCA and lower CAH values than PDMS-*b*-AC, presumably due to the incorporation of the more hydrophobic DFHMA blocks and crosslinking. The highest WCA value and the minimal CAH were detected for PDMS-*b*-FPAC due to the

synergistic effect of the hydrophobic DFHMA blocks and MAPOSS. The θ_a appeared to increase slightly, while the θ_r increased notably. It was suggested that the increased surface roughness generated by MAPOSS had a major effect on WCA and CAH. Compared with the polyacrylate-*b*-PDMS samples, PMTFPS-*b*-AC had minimum WCA and maximum CAH. Morphology with no clearly microphase separation and the smallest nano-scaled roughness demonstrated by AFM would be reasons for the wettability of PMTFPS-*b*-AC film.

Ice Shear Strength

The values of ice shear strength on the copolymer films are shown in Fig. 6. The higher content of the fluorine might be not suitable for anti-icing because it could enhance the interaction between surface and water[22]. Hence, higher fluorine content in PDMS-*b*-FAC and PMTFPS-*b*-AC samples demonstrated by XPS may be a reason for their higher ice shear strength than PDMS-*b*-AC and PDMS-*b*-FPAC. It could be noticed that the ice shear strength of PDMS-*b*-FPAC containing MAPOSS units decreased drastically and held the lowest value (145 ± 13) kPa among all samples. In fact, POSS could facilitate microphase separation of the copolymers and increase the nano-scaled roughness, which was coincident well with the analysis about distinct multiphase detected by AFM. Bigger nano-scaled surface roughness brought about lower ice shear strength partly. Furthermore, introducing POSS could possibly improve the anti-icing and anti-frosting properties by increasing the water contact angle or decreasing contact angle hysteresis, which was in agreement with the previous studies on high-WCA and low-CAH surfaces[11, 23]. Significantly, the POSS-containing fluorosilicone block copolymers combined the advantages of POSS, PDMS and fluoropolymers synergistically in an appropriate way and they may have deicing performance under a nature force.

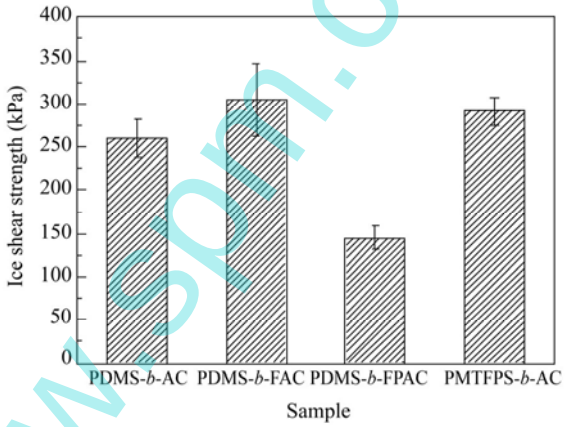

Fig. 6 Ice shear strength of fluorosilicone acrylate copolymers films

CONCLUSIONS

Two series of fluorosilicone block copolymers were synthesized *via* polymerization of acrylates by employing PDMS and PMTFPS as macroazoinitiators, respectively. Characterizations of morphology, surface chemical composition and water contact angles suggested that the fluorosilicone chains aggregated on the top of the polymer surfaces and the nano-scaled surface roughness increased, caused by microphase separation. Assessed by water contact angle measurement and ice shear strength, PDMS-*b*-FPAC with MAPOSS component exhibited better icephobic performance and hydrophobic properties. Therefore, the fluorosilicone block copolymers have the advantage of silicone and fluoropolymers, and could be potentially applied in functional icephobic coatings.

REFERENCES

1 Menini, R. and Farzaneh, M., J. Adhes. Sci. Technol., 2011, 25: 971
2 Susoff, M., Siegmann, K., Pfaffenroth, C. and Hirayama, M., Appl. Surf. Sci., 2013, 282: 870
3 Guo, P., Zheng, Y., Wen, M., Song, C., Lin, Y. and Jiang, L., Adv. Mater., 2012, 24(19): 2642
4 Arianpour, F., Farzaneh, M. and Kulinich, S. A., Appl. Surf. Sci., 2013, 265: 546
5 Antonini, C., Innocenti, M., Horn, T., Marengo, M. and Amirfazli, A., Cold Reg. Sci. Technol., 2011, 67: 58
6 Cao, L.L., Jones, A.K., Sikka, V.K., Wu, J.Z. and Gao, D., Langmuir, 2009, 25: 12444
7 Kulinich, S.A., Farhadi, S., Nose, K. and Du, X.W., Langmuir, 2011, 27(1): 25
8 Chen, J., Liu, J., He, M., Li, K., Cui, D., Zhang, Q., Zeng, X., Zhang, Y., Wang, J. and Song, Y., Appl. Phys. Lett., 2012, 101(11): 111603
9 Nosonovsky, M. and Hejazi, V., ACS Nano, 2012, 6(10): 8488
10 Jung, S., Dorrestijn, M., Raps, D., Das, A., Megaridis, C. M. and Poulikakos, D., Langmuir, 2011, 27 (6): 3059
11 Yu, D., Zhao, Y., Li, H., Qi, H., Li, B. and Yuan, X., Prog. Org. Coat., 2013, 76(10): 1435
12 Wei, X., Jia, Z., Sun, Z., Liao, W., Qin, Y. and Guan, Z., IEEE Transactions on, 2012, 19(6): 2063
13 Zhu, L., Xue, J., Wang, Y., Chen, Q., Ding, J. and Wang, Q., ACS Appl. Mater. Inter., 2013, 5(10): 4053
14 Li, J., Zhao,Y., Hu, J., Shu, L. and Shi, X., J. Adhes. Sci. Technol., 2012, 26: 665
15 Yang, S., Xia, Q., Zhu, L., Xue, J., Wang, Q. and Chen, Q., Appl. Surf. Sci., 2011, 257(11): 4956
16 Yi, L., Huang, C. and Zhou, W., J. Polym. Sci., Part A: Polym. Chem., 2012, 50(9): 1728
17 Meraa, A.E., Goodwin, M., Pike, J.K. and Wynne, K.J., Polymer, 1999, 40: 419
18 Liang, J., He, L., Dong, X. and Zhou, T., J. Colloid Interf. Sci., 2012, 369(1): 435
19 Guan, C.M., Luo, Z.H., Qiu, J.J. and Tang, P.P., Eur. Polym. J., 2010, 46(7): 1582
20 Uragmi, T., Yamada, H. and Miyata, T., Macromolecules, 2006, 39: 1890
21 Lian, K.J., Chen, C.Q., Liu, H., Wang, N.X., Yu, H.J. and Luo, Z.H., J. Appl. Polym. Sci., 2011, 120(1): 156
22 Murase, H., Nanishi, K., Kogure, H., Fujibayashi, T., Tamura, K. and Haruta, N., J. Appl. Polym. Sci., 1994, 54: 2051
23 Meuler, A.J., Smith, J.D., Varanasi, K.K., Mabry, J.M., Mckinley, G.H. and Cohen, R.E., ACS Appl. Mater. Inter., 2010, 2: 3100